PRAMANA
— journal of
physics

Vol. 53, No. 2
August 1999
pp. 341–351

Local canted spin behaviour in $Co_{1.4-x}$ $Zn_xGe_{0.4}$ $Fe_{1.2}O_4$ spinels: A macroscopic, mesoscopic and microscopic study

M V SUBBARAO*, S M YUSUF†, R G KULKARNI* and L MADHAV RAO‡

*Department of Physics, Saurashtra University, Rajkot 360 005, India

†Condensed Matter Physics Division, Bhabha Atomic Research Centre, Trombay, Mumbai 400 085, India

‡Inter University Consortium for DAE Facilities, Bhabha Atomic Research Centre, Mumbai 400 085, India

†Author for correspondence

MS received 9 October 1998; revised 2 March 1999

Abstract. DC magnetization, neutron depolarization and neutron diffraction (with both polarized and unpolarized neutrons) measurements have been reported for the $Co_{1.4-x}Zn_xGe_{0.4}Fe_{1.2}O_4$ spinels with $x = 0.5$, 0.6 and 0.7. Neutron depolarization and neutron diffraction measurements confirm the presence of a long range ferrimagnetic ordering of the local canted spins in these ferrite samples. The observed features of low field magnetization have been explained under the framework of thermally activated domain wall movement of ferrimagnetic arrangement of local canted spins. An important role of magnetic anisotropy (due to the presence of Co^{2+} ions) in establishing the magnetic ordering and domain kinetics in these ferrites has been observed.

Keywords. Ferrites; local canted spins; magnetic anisotropy; domain wall pinning.

PACS Nos 75.25.+z; 75.30.Gw; 75.60.-d

1. Introduction

The magnetic structures of the spinel ferrites depend upon the types of magnetic ions residing on the tetrahedral (A) and octahedral (B) sites and the relative strengths of the inter-(J_{AB}) and intra-sublattice interactions (J_{AA}, J_{BB}). Generally all the three exchange interactions, viz J_{AA}, J_{BB} and J_{AB} are negative. Further, when all the metal ions (cations) are magnetic, usually the inter-sublattice interaction J_{AB} is the strongest with $|J_{AB}| >> |J_{BB}| > |J_{AA}|$. Thus, J_{AB} renders the undiluted spinel as ferrimagnetic with A-site moments aligned antiparallel to the B-site moments keeping the AA and BB bonds unsatisfied. Selective magnetic dilution of A and B sites accentuates the competition between the various exchange interactions resulting in a wide spectrum of magnetic ordering ranging from ferrimagnetism, antiferromagnetism, local canted spin (LCS) to semi-spin glass (SSG), spin glass (SG) etc. [1]. A quantitative phase diagram was proposed by Villain [2] that predicts ferrimagnetic, SSG and SG ground states as the magnetic dilution

progresses. The presence of some selective magnetic ions such as Co^{2+} in ferrite systems introduces an additional factor, i.e. uniaxial anisotropy [3] which may complicate the magnetic phase diagram [4].

Recent low-field and high-field magnetization, ac susceptibility and Mossbauer measurements [5, 6] down to 90 K on $Co_{1.4-x}Zn_xGe_{0.4}Fe_{1.2}O_4$ with $x = 0.4$, 0.5, 0.6 claimed to have seen the signatures of local spin canting behavior with the absence of long range ferrimagnetic ordering. Since neutrons can give unambiguous answers to the question of the presence or absence of long range magnetic ordering, we have studied three compositions (x = 0.5, 0.6 and 0.7) in the $Co_{1.4-x}Zn_xGe_{0.4}Fe_{1.2}O_4$ series. We have supplemented our neutron diffraction studies with dc magnetization and neutron depolarization measurements.

2. Experimental details

The polycrystalline samples of the spinel series $Co_{1.4-x}Zn_xGe_{0.4}Fe_{1.2}O_4$ with x = 0.5, 0.6 and 0.7 were prepared by the usual double sintering ceramic method. The starting materials were analytical reagent grade Fe_2O_3 (Thomas Baker), CoO (Thomas Baker), ZnO (E Merk) and GeO_2 (E Merk). The oxides (Fe_2O_3, CoO, ZnO, GeO_2) were mixed in stoichiometric proportions and pre-sintered at 990 °C for 12 h. In the final sintering process the material was held at 1050°C for 12 h and slowly cooled to room temperature (2 °C/min). All three samples were characterized by x-ray diffraction at room temperature. The theoretical stoichiometries of all three samples were confirmed by Rietveld refinement of room temperature (300 K) neutron diffraction patterns of all the three samples with site occupancies as varied parameters in the refinement process. The compositional homogeneity of the samples was also ascertained by energy-dispersive X-ray mapping of some regions of all the three samples.

The zero-field-cooled (ZFC) and field-cooled (FC) dc magnetization measurements were carried out on the x = 0.6 and 0.7 samples using a quantum design SQUID magnetometer (model MPMS) using the same procedure as described in our earlier paper [4]. The ZFC and FC measurements were carried out over the temperature range 5–300 K and with fields 30 Oe and 10 Oe for the x = 0.6 and 0.7 samples, respectively.

The one-dimensional (1D) neutron-depolarization measurements on the $x = 0.6$ and 0.7 samples were carried out using the neutron-polarization analysis spectrometer (PAS) at Dhruva reactor, Trombay ($l = 1.201$ Å). The incident neutron beam polarization is 0.9883(1). The detailed description of the spectrometer has been given in earlier papers [7,8]. The temperature of sample was varied between 11 and 300 K in a closed-cycle helium refrigerator and controlled to better than 0.1 K. The ZFC and FC neutron-depolarization measurements (with the same field values as applied for the ZFC and FC magnetization measurements) were carried out using the same procedure [9] as used for the present ZFC and FC magnetization measurements. In neutron depolarization experiments the amount of depolarization depends on the mean domain size δ, domain magnetic induction B, neutron wavelength λ and the average number of domains N along the path of neutrons ($N = d/\delta$, where d is the effective sample thickness) [8]. The samples studied here are of arbitrary effective thickness. Hence no quantitative comparison between the transmitted neutron beam polarization P values of different samples can be made. However, the recorded data would be good enough to find the nature of magnetic ordering.

The unpolarized neutron diffraction patterns for all the three samples were recorded at 300 K and 11 K over the angular range of 10–70°. The temperature dependence of (111) Bragg peak intensity measurements for x = 0.5 sample using unpolarized neutrons and for x = 0.6 and 0.7 samples using polarized neutrons, were carried out over the temperature range 11–300 K. The flipping ratio (R) measurements of (220), (222) and (111) Bragg reflections for x = 0.6 and 0.7 samples were carried out at 11 K.

All measurements were carried out on compacted powdered samples. Compacting ensures that rotation of the crystallites does not take place.

3. Experimental results and data analysis

3.1 DC magnetization measurements

Figures 1 and 2 show the temperature dependence of the ZFC and FC magnetization for $x = 0.6$ and 0.7 samples, respectively. The ZFC and FC curves bifurcate at about 300 K for both the samples with $x = 0.6$ and $x = 0.7$ (figures 1 and 2). The ZFC curves show broad maxima at about 110 K and 120 K for the $x = 0.6$ and 0.7 samples, respectively. It is to be noted that the ZFC magnetization curves (figures 1 and 2) show asymmetric behavior. The FC magnetization continuously increases for both the $x = 0.6$ and 0.7 samples with the lowering of temperature until about 100 K; thereafter it decreases substantially for the $x = 0.6$ sample and marginally decreases for the $x = 0.7$ sample.

3.2 Neutron diffraction measurements

The Bragg reflection intensity formulae used for both unpolarized neutrons and polarized neutrons are taken from ref. [10]. In case of unpolarized neutrons, the Bragg reflection

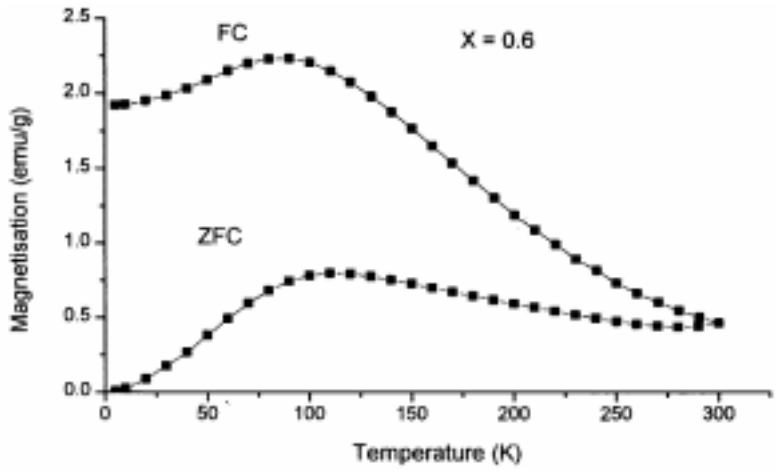

Figure 1. ZFC and FC magnetization as a function of temperature for the $x = 0.6$ sample with 30 Oe applied field.

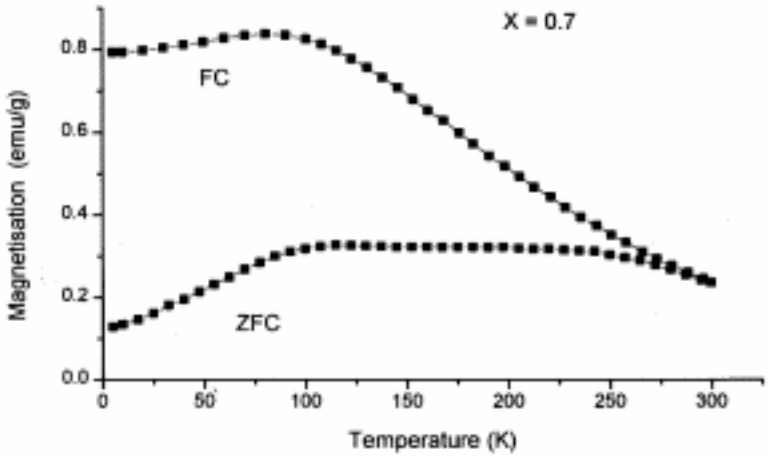

Figure 2. ZFC and FC magnetization as a function of temperature for the $x = 0.7$ sample with 10 Oe applied field.

intensity in absence of an external magnetic field is given by the formula

$$I^0_{hkl} = \text{constant } j\ L(N^2 + 2/3M^2)\exp(-2W) \tag{1}$$

for a cubic polycrystalline ferrimagnet with both chemical and magnetic long range ordering, where j is the multiplicity of the plane (hkl), L is the Lorentz factor, N and M the nuclear and magnetic structure amplitudes and exp$(-2W)$ is the Debye–Waller factor. For polarized neutrons with polarization parallel (+) and antiparallel $(-)$ relative to the magnetization of the sample, on the other hand, the Bragg intensities are given by the formulae

$$I^+_{hkl} = \text{constant } j\ L(N^2 + M^2 + 2PDNM)\exp(-2W) \tag{2}$$

and

$$I^-_{hkl} = \text{constant } j\ L(N^2 + M^2 - 2PD(2f-1)NM)\exp(-2W). \tag{3}$$

The cross terms in the parenthesis arise from the coherence between the nuclear and magnetic scattering processes in the case of polarized neutrons. Here P is the incident beam polarization, D is the polarization transmission through the sample, and f is the neutron polarization reversal efficiency of the RF flipper. It is evident that polarized neutron diffraction essentially measures the interference between nuclear scattering and magnetic scattering and therefore is very sensitive to the presence of very small ordered magnetic moments in the lattice.

The unpolarized neutron diffraction data for all the three samples taken at 300 K (paramagnetic region), were analysed using the Rietveld refinement technique [11]. It is observed that Zn-ions have a very strong A-site preference. The analysis reveals that the A-site magnetic ion concentration (c_A) for x = 0.5, 0.6 and 0.7 compositions are 0.19(1), 0.17(1) and 0.14(1), respectively which are well below the site percolation threshold [12] c_P = 0.429. For each composition the remaining magnetic ions occupy the B-sites.

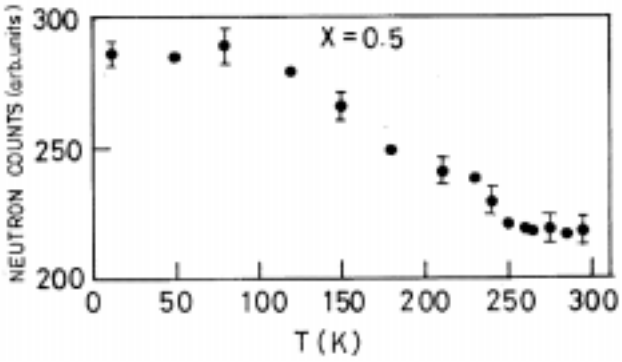

Figure 3. The temperature dependence of (111) Bragg peak intensity (for unpolarized neutrons) for the $x = 0.5$ ferrite.

The unpolarized neutron diffraction study for $x = 0.5$ ferrite also revealed that the intensities of (111), (220) and (222) inner Bragg reflections increase significantly with lowering of temperature, indicating strong magnetic contributions to these reflections. No broadening of the half widths of these Bragg reflections were observed with enhancement of their intensities, indicating that the ordered moments have long range correlations. As an illustration, the temperature dependence of the (111) Bragg peak intensity is shown in figure 3. From this figure the Neel temperature was estimated to be around 255 K. The unpolarized neutron diffraction patterns for x = 0.6 and 0.7 showed no observable increase in the intensities of inner Bragg reflections as one lowers the temperature down to 11 K. As stated earlier, in such situations one takes recourse to polarized neutrons which are very sensitive probes capable of measuring very small magnetic contributions to the nuclear Bragg peaks quite accurately. The peak intensities I^+ and I^- of the inner Bragg reflections for the two states of neutron polarization were measured as a function of temperature for the x = 0.6 and 0.7 compositions. It may be remarked that I^+ will be equal to I^- in the absence of an ordered moment contribution to the Bragg intensity. Figures 4 and 5 show the I^+ variation of the (111) Bragg peak as a function of temperature. From figure 4 the Neel temperature is estimated to be around 255 K for x = 0.6. From figure 5 it is difficult to estimate the Neel temperature for the x = 0.7 sample. The temperature dependence of Bragg peak intensity for the x = 0.7 sample (figure 5) is very much different from the usual behaviour as seen for the other two samples (figures 3 and 4). The half widths of the relevant inner Bragg reflections remain unchanged throughout the temperature range explored.

The ordered site moments for x = 0.5 were obtained from the unpolarized neutron diffraction data, taken at 11 K ($T_N \approx 255$ K). The A-site magnetic moment is calculated by selecting (220) reflection (whose magnetic contributions depends only on A-site magnetic moment) and B-site by (222) reflection (whose magnetic contributions depends only on B-site magnetic moment). The magnetic contributions to the Bragg intensity of the (111) and (400) reflections come from both A and B site moments. Reflections like (111) or (400) were used to cross check the correctness of the site-moment values obtained. On the other hand, the ordered site moments for x = 0.6 and 0.7 were obtained from the polarized neutron diffraction data taken at 11 K (well below the Neel temperature), by using the flipping ratio method [13]. The polarization ratio or flipping ratio, R, is the ratio

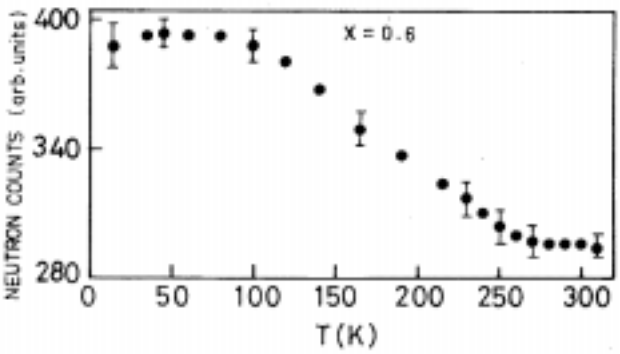

Figure 4. The temperature dependence of (111) Bragg peak intensity (I^+) for the $x = 0.6$ ferrite.

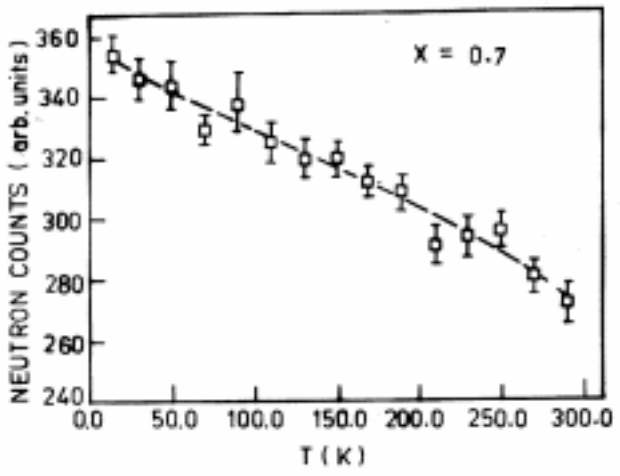

Figure 5. The temperature dependence of (111) Bragg peak intensity (I^+) for the $x = 0.7$ ferrite. The broken line is drawn to guide the eye.

of the intensities for a particular reflection for two incident neutron spin states (given by equations (2) and (3)), and is as follows

$$R_{hkl} = \frac{I^+_{hkl}}{I^-_{hkl}} = \frac{N^2 + M^2 + 2PDNM}{N^2 + M^2 - 2PD(2f-1)NM} = \frac{1 + \gamma^2 + 2PD\gamma}{1 + \gamma^2 - 2PD(2f-1)\gamma}$$

$$\text{where } \gamma = M/N. \tag{4}$$

This equation (4) can be used to get γ and hence M. The A-site and B-site moments are calculated from the flipping ratio measurements of (220) and (222) reflections, respectively. These values were cross checked by calculating the expected flipping ratio for the (111) reflection and comparing it with the observed one. The agreement

Table 1. Tetrahedral and octahedral site moments of $Co_{1.4-x}Zn_xGe_{0.4}Fe_{1.2}O_4$ ferrites obtained from neutron diffraction studies.

x	Site moment (μ_B) at 11 K			
	A-site		B-site	
	Expt.	Free ion	Expt.	Free ion
0.5	0.64(5)	0.65(2)	2.54(5)	4.02(2)
0.6	0.12(6)	0.59(2)	0.04(6)	3.90(2)
0.7	0.42(6)	0.48(2)	0.14(6)	3.81(2)

between these values was quite satisfactory. The measured site moments at 11 K and theoretical free-ion spin only site moments for all the three samples are summarized in table 1. It is evident from table 1, that the A-site moments are closer to their theoretical free-ion values (except for x = 0.6 composition), suggesting that A-site moments are highly collinear for x = 0.5 and 0.7 samples. On the other hand, for all the three samples B-site moments are much smaller than their free-ion values, indicating that the B-site moments are highly non-collinear.

In the spinel structure, if the magnetic moments are all ordered collinearly (Neel ordering) then one expects the ordered site moments deduced from the normal Bragg reflections such as (111), (220), (222) to be close to the estimated free-ion moments since, in such a situation, the moments of the magnetic ions will be fully aligned along the longitudinal direction (i.e. along the axis of broken symmetry). On the other hand, if the magnetic ordering is noncollinear, the ordered site moments deduced from the normal Bragg reflections will correspond only to the longitudinal components since the transverse components do not contribute to the intensities of these Bragg reflections. Spatial ordering of the transverse magnetic components gives rise to the (200) Bragg reflection which is purely magnetic. The site moments listed in table 1 derived from the Bragg reflections therefore correspond to the longitudinal components of the ordered moment. The complete absence of the (200) magnetic Bragg reflection for all the three compositions indicates that the transverse components, which are quite large in magnitude, are spatially completely disordered.

3.3 Neutron depolarization measurements

The temperature dependence of zero field cooled (ZFC) and field cooled (FC) transmitted neutron beam polarization P for x = 0.6 with a field of 30 Oe and for x = 0.7 with a field of 10 Oe are depicted in figures 6 and 7, respectively. The procedure of obtaining P values from the measured flipping ratios for the transmitted polarized beam is described elsewhere [9]. For the x = 0.6 sample, both ZFC transmitted polarization and FC transmitted polarization show a continuous decrease right from 300 K and attain a constant value below about 100 K. The deviation between the ZFC and FC depolarization starts below about 260 K and the deviation increases with decreasing temperature. From figure 6, it is evident that, in the FC case a higher depolarization is observed than in the ZFC case, which contradicts the normal situation, where one would expect more depolarization in the ZFC case than in the FC case. The x = 0.7 sample also shows (figure 7) a continuous decrease in both ZFC

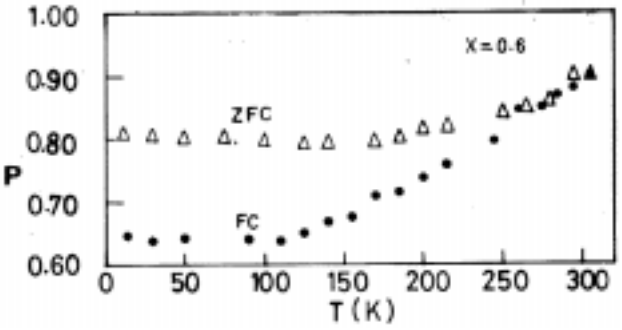

Figure 6. ZFC and FC transmitted beam polarization P as a function of temperature measured in a 30 Oe field for the $x = 0.6$ ferrite.

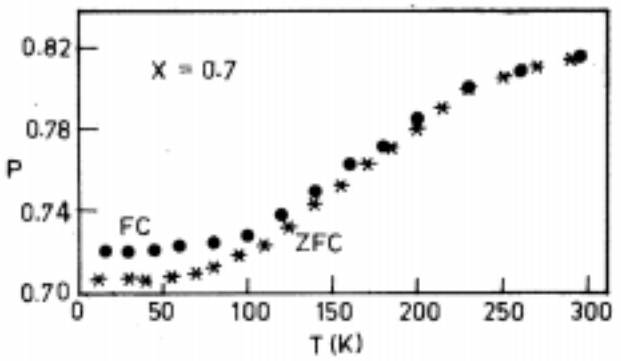

Figure 7. ZFC and FC transmitted beam polarization P versus temperature measured in a 10 Oe field for the $x = 0.7$ ferrite.

and FC transmitted polarization right from 300 K and attain a constant value below 50 K. A deviation between the ZFC and FC depolarization starts below about 220 K. It is also seen that, a higher depolarization is observed for the ZFC case than the corresponding FC case, as expected.

4. Discussion

Figure 1 shows that the broad peak in the ZFC and FC magnetization curves occurs at the same temperature where a broad peak in the χ_{ac} curve [5] was observed. A strong irreversibility between the ZFC and FC magnetization occurs for all the three samples (figures 1 and 2 and also see ref. [5]). Such characteristic behaviors in χ_{ac} and ZFC–FC magnetization have been observed in spin-glass or spin-glass like materials [14,15]. However, for systems where long-range order is involved, such features can arise from domains, domain walls and also from disorder. In LCS systems such characteristic behaviors have been interpreted in terms of kinetic freezing of magnetic domains [1,4,9]. In order to identify the nature which the present materials possess some further clues are needed. Microscopic neutron diffraction results provide help.

For all three samples the presence of long-range ferrimagnetic ordering is confirmed from the presence of magnetic Bragg contributions to the fundamental inner reflections over all temperatures below the Neel temperature $T_{\rm N}$ (figures 3–5). It is seen in table 1 that the B-site moments are much smaller than their theoretical free-ion moment values for all the three samples, indicating that the B-site moments are highly non-collinear. For $x = 0.6$ sample, the A-site moment is also highly non-collinear. As (200) Bragg peak was not observed at low temperature diffraction patterns for any one of the samples, the possibility of any uniform canting relative to the average magnetization (Yafet–Kittel-type structure [16]) is ruled out. In brief, neutron diffraction study confirms local (random) canting of spins with ferrimagnetic long-range ordering of longitudinal spin components.

The neutron depolarization study on both x = 0.6 and 0.7 samples shows the existence of magnetic domains and is consistent with the neutron diffraction results, namely a long-range ferrimagnetic ordering of longitudinal spin components. It is interesting to note that the depolarization persists at temperatures well above the $T_{\rm N}$ value obtained from the neutron diffraction measurements. This could be explained due to formation of smaller domains/clusters at temperatures above $T_{\rm N}$. The $T_{\rm N}$ values estimated from the neutron diffraction measurements correspond to the onset of true long range ferrimagnetic ordering of spins. However, the depolarization study do indicate the presence of smaller domains at temperatures higher than $T_{\rm N}$ obtained from the diffraction measurements. We therefore, do not see the expected trend between the $T_{\rm N}$ value obtained from neutron diffraction experiments and magnetic dilution x. For both the samples, a continuous drop of both ZFC and FC transmitted neutron beam polarization P right from 300 K down to about 100 K for x = 0.6 and about 50 K for x = 0.7 sample (below which P attains respective constant values) indicates no breakdown of ferrimagnetic-like domain structures. The observed irreversibility between the ZFC and FC depolarization curves clearly shows that the domain mobility strongly depends upon the cooling process of the samples.

Hence, the presence of ferrimagnetic domains are confirmed from both mesoscopic neutron depolarization and microscopic neutron diffraction studies. The above discussion shows that the characteristic behaviours observed in low field magnetization (figures 1 and 2) do not result from a breakdown of ferrimagnetic correlation or a transition to any spin glass-like phase but can be related to magnetic domain effects [9]. From our ZFC–FC magnetization and depolarization studies it is apparent that the growth and/or kinetic freezing mechanisms of magnetic domains depend on the exact cooling conditions (i.e. ZFC or FC) and also on the composition. In a normal situation, when the sample is cooled in the absence of a field (ZFC case), the domains are more random and as a result the effective depolarizing internal field (the transverse field seen by the incident polarized neutron beam) is high which causes more depolarization in the ZFC case than in the FC case [9]. This is the situation for the x = 0.7 sample. In the samples which we have studied here, Co^{2+} can introduce uniaxial anisotropy [3] and in such a situation very large domains can be maintained in the FC case as compared to the ZFC case [4,9]. Hence, the observed higher depolarization in the FC case as compared to the ZFC case for the Co^{2+} rich x = 0.6 sample as compared to x = 0.7 sample can be related to the effect of the presence of a higher uniaxial anisotropy. It is observed that the bifurcation temperatures between the FC and ZFC data curves are different for the two types of measurements namely, neutron depolarization and low field dc magnetization. Here it is to be recalled that the neutron depolarization is a mesoscopic probe with a typical probing length scale of 100 Å to a few thousand angstroms. On the other hand, magnetization study probes sample on a macro-

scopic length scale. Therefore, the bifurcation arising from magnetic domain effects need not be identical in two length scales of measurements. Moreover, it has been observed that the FC–ZFC branching is strongly field dependent in this type of ferrite systems [4]. Hence, any small variation in applied field values in two different measurements can cause a significant change of branching temperature.

The site ordered longitudinal moments observed from neutron diffraction studies at 11 K (table 1) for the $x = 0.6$ sample is less as compared to the other two samples. This indicates that for $x = 0.6$ sample canting angle is large for both the sites. It has already been discussed that our neutron diffraction study confirms local (random) canting of spins with ferrimagnetic long-range ordering of longitudinal spin components (LCS structure). The amount and nature of canting depends upon the distribution of magnetic atoms in A and B-sites and the relative strength of J_{AA}, J_{BB} and J_{AB} interactions. Moreover, a possible presence of random uniaxial anisotropy due to the Co^{2+} ions in these systems may complicate the nature of ordering [3,4,9]. However, at present we do not have any clear explanation as to why the canting angle is large for the sample with $x = 0.6$.

The domain wall pinning does take place in these ferrites and can be clearly seen in figures 1–2 and 6–7. The peaking of χ_{ac} observed by earlier workers [5] and our ZFC magnetization and FC magnetization can be explained in the following way. At lower temperature, a higher value of magnetization is expected in the ferrimagnetically ordered state due to ordering of spins within the domains, and the magnetic hardness also shows a higher value because of domain-wall pinning. These two have opposite effects on the temperature dependence of magnetization and shows up as a peak in the χ_{ac} and low field dc magnetization curves.

5. Summary and conclusion

We have performed magnetic studies in different length scales such as macroscopic (low field magnetization), mesoscopic (low field neutron depolarization) and microscopic (polarized and unpolarized neutron diffraction) on $Co_{1.4-x}Zn_xGe_{0.4}Fe_{1.2}O_4$ spinels with $x = 0.5$, 0.6 and 0.7. Our neutron depolarization and neutron diffraction measurements clearly establish the presence of long range ferrimagnetic ordering of local (random) canted spins in all the three samples. The observed temperature-dependent features of low field ZFC and FC magnetization have been explained, with the help of neutron depolarization and neutron diffraction data, in terms of the thermally activated domain wall movement in a LCS arrangement. The Co^{2+} ions in these ferrite systems introduce uniaxial anisotropy. The effect of such an anisotropy on the magnetic ordering has been brought out.

Acknowledgement

The authors are grateful to T V Chandrasekhar Rao for collecting magnetization data on the SQUID magnetometer. Financial assistance for this project from the Inter-University Consortium for DAE Facilities, Indore is gratefully acknowledged.

References

[1] J L Dormann and M Nogues, *J. Phys. Condens. Matter* **2**, 1223 (1990)
[2] J B Villain, *Z. Phys*. **B33**, 31 (1979)

[3] J B Goodenough, *Magnetism and the chemical bonds* (New York, Wiley, 1963)
[4] S M Yusuf, V C Sahni and L Madhav Rao, *J. Phys. Condens. Matter* **7**, 873 (1995)
[5] J Nogues, T Puig, R B Jotania, R V Upadhyay, R G Kulkarni and K V Rao, *J. Magn. Magn. Mater.* **99**, 275 (1991)
[6] R B Jotania, R V Upadhyay and R G Kulkarni, *IEEE Trans. Magn.* **28**, 1889 (1992)
[7] L Madhav Rao, S M Yusuf and R S Kothare, *Indian J. Pure Appl. Phys.* **30**, 276 (1992)
[8] S M Yusuf and L Madhav Rao, *Pramana – J. Phys.* **47**, 171 (1996)
[9] S M Yusuf and L Madhav Rao, *J. Phys. Condens. Matter* **7**, 5891 (1995)
[10] L Madhav Rao, *Bull. Mater Sci*. **7**, 303 (1995)
[11] H M Rietveld, *J. Appl. Crystallogr*. **2**, 65 (1969)
[12] F Scholl and K Binder, *Z. Phys*. **B39**, 239 (1980)
[13] C G Shull and R Nathans, *Phys. Rev. Lett.* **19**, 384 (1969)
[14] C Y Huang, *J. Magn. Magn. Mater*. **51**, 1 (1985)
[15] J L Soubeyroux, Fiorani and E Agostinelli, *J. Magn. Magn. Mater*. **54–57**, 83 (1986)
[16] N S Satya Murthy, M G Netera, S I Youssef, R J Begum and C M Srivastava, *Phys. Rev.* **181**, 969 (1969)